Polym Int 54:939–945 (2005)
DOI: 10.1002/pi.1793

Nanocomposites of poly[(butylene succinate)-*co*-(butylene adipate)] (PBSA) and twice-functionalized organoclay

Guangxin Chen and Jin-San Yoon*
Department of Polymer Science and Engineering, Inha University, Incheon 402-751, Korea

Abstract: A new method is described to prepare composites of poly[(butylene succinate)-*co*-(butylene adipate)] (PBSA) with an organophilic clay having a particular functional group, namely twice-functionalized organoclay (TFC). TFCs were produced by treating Cloisite 25A® with (glycidyloxypropyl)trimethoxy silane (GPS) or (methacryloyloxypropyl)trimethoxy silane (MPS). Reaction of the silane compound with the organoclay surface was monitored by Fourier-transform infrared spectroscopy (FTIR). PBSA composites with the three different clays were prepared successfully via melt mixing. The *d* spacing and the morphology of the composites were monitored by X-ray diffraction and by transmission electron microscopy. The linear storage modulus of the composites in the melt state increased significantly as a result of incorporation of TFC. Tensile modulus and strength at break of PBSA/TFC–GPS and those of PBSA/TFC–MPS were far superior to those of PBSA/C25A.

Keywords: poly[(butylene succinate)-*co*-(butylene adipate)]; twice functionalized; silane compounds; nanocomposites; clays; (glycidyloxypropyl)trimethoxy silane; (methacryloyloxypropyl)trimethoxy silane

INTRODUCTION

Silicate-layered polymer nanocomposites have recently been the focus of both academic and industrial attention[1,2] because they often have greatly enhanced physical and/or chemical properties, even with small amounts of silicate present, compared with the conventional micro-scale composite materials. These unique properties of polymer/silicate nanocomposites come from: (1) the high degree of dispersion; and (2) the strong interactions between the silicate layers and the polymer matrix[3] as a result of the high interfacial surface-to-volume ratio.[4]

Since clays, which consist of a stacked structure of parallel silicate layers, usually lack in affinity to polymer matrices, the interlayer cations between the silicate layers, such as Na^+, Ca^{2+} or K^+ are exchanged with organic cations to increase the organophilicity of the clay layers. This lowers the interfacial energy and improves wetting with the polymer matrix.[5]

A significant amount of research has been carried out to improve compatibility between the inorganic component and the polymer matrix because the properties of the nanocomposites depend strongly on the extent to which the organic and inorganic phases are made compatible.[5]

If the organophilic clay has functional groups which can react with the polymer matrix, a higher degree of dispersion of the clay layers can be achieved to give nanocomposites with advanced physical properties. However, little attention has been paid up to now to nanocomposites composed of silicates having special functional groups.

In this study, we devised a new and convenient method to introduce additional functional groups to the clays which have already been modified with $[(CH_3)_2HTN^+ (C_8H_{17})]$, where T is hydrogenated tallow consisting of ca 65% C18; 30% C16; 5% C14, ie Cloisite 25A®, as shown in Fig 1. We call the product from this process clay twice-functionalized organoclay (TFC). TFC was prepared by reacting the silane compounds $[Si(OR)_xR'_{4-x}]$ with the silanol groups of the original organoclay.

The organophilicity of TFC should be much higher than that of Cloisite 25A (C25A). Composites were prepared by compounding poly[(butylene succinate)-*co*-(butylene adipate)] (PBSA) with TFC. The newly synthesized TFC is expected to interact more strongly with PBSA than C25A due to the higher organophilicity and due to the reaction between the functional groups of TFC and PBSA.

EXPERIMENTAL

Materials

Poly[(butylene succinate)-*co*-(butylene adipate)] (PBSA) was obtained from the Irae Chemical Co,

* Correspondence to: Jin-San Yoon, Department of Polymer Science and Engineering, Inha University, Incheon 402-751, Korea
E-mail: jsyoon@inha.ac.kr
Contract/grant sponsor: Interdisciplinary Research Program of the KOSEF; contract/grant number: R01-2002-000-00146-0
(*Received 13 September 2004; revised version received 10 November 2004; accepted 13 December 2004*)
Published online 28 February 2005

 Polym Int 0959–8103/2005/$30.00

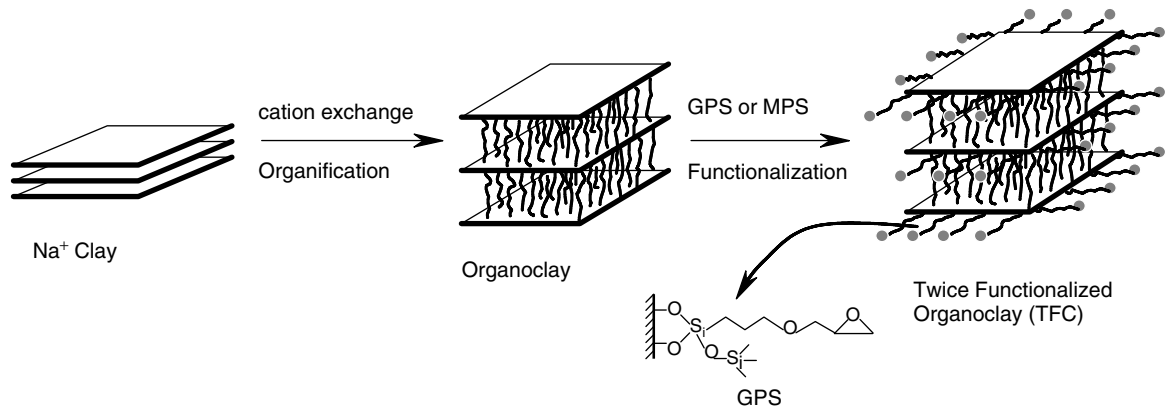

Figure 1. Schematic diagrams for preparation of the twice-functionalized organoclay (TFC).

Korea, with a molecular weight of 5×10^{-4} g mol^{-1} as reported by the manufacturer, and was dried in a vacuum oven for at least 2 days at 50 °C. The organically modified clay (organoclay), C25A, was purchased from Southern Clay Product Inc and was purified by dissolution in ethanol at 70 °C for 4 h to remove any contaminations. Two types of silane coupling agents, (glycidyloxypropyl)trimethoxy silane (GPS) and (methacryloyloxypropyl)trimethoxy silane (MPS), were supplied by Aldrich.

Synthesis of twice-functionalized organoclay (TFC)

After 3.5 g of the silane coupling agent (GPS or MPS) was hydrolyzed at pH 4.0 for 4 h with acetic acid in ethanol/deionized water (9/1 wt/wt) mixture, 10 g of C25A was added and then the mixture was heated with reflux at 70 °C for different reaction times. At the end of the reaction, the mixture was allowed to cool down with stirring. The reaction product was diluted with n-propanol fivefold to remove the soluble homocondensates, then filtered and repeatedly washed with ethanol at room temperature. The product was dried in an oven under a vacuum at 50 °C for at least 48 h. Figure 1 is the schematic diagram for the preparation of the twice-functionalized organoclay (TFC). The chemical reaction between Cloisite 25A and the silane compounds takes place mainly on the edge of the silicate layers where the concentration of the silanol groups is much higher than that on the plain surface.[6] The grafted amount of the epoxy groups on organoclay was determined as 0.36 mmol g^{-1} by the chemical titration method.[7]

Preparation of the composites

Nanocomposites of PBSA/clay were prepared by melt compounding of PBSA with the clays at 160 °C for 6 min. C25A and both twice-functionalized organoclays (TFC–GPS and TFC–MPS) were used. The organoclays in powder shape were dispersed in methanol (10 g ml^{-1}) and sonicated for 10 min. Then, the solution was scattered over PBSA pellets and was dried in a vacuum oven for 12 h at 40 °C. The mixture was melt compounded by using a Brabender internal mixer at 160 °C. The compounded and pelletized strands were dried under vacuum at 50 °C to remove residual water. The dried pellets were then hot-pressed at 160 °C for 1 min under 4 atm to prepare sheets with a thickness of about 0.5 mm. It should be noted that sample names are given with respect to the %w/w of silane coupling agent-treated clay and the copolymer; for example, PBSA/TFC–GPS10 is PBSA mixed with 10 % wt/wt TFC–GPS.

Characterization

Grafting behavior of the silane coupling agents was monitored by using a Bio-Rad Fourier-transform infrared (FTIR) spectrophotometer. Determination of the quantity of the bonded coupling agent was assessed by FTIR measurement through the intensity of the Sibond;OH peak. For this purpose, KBr pellets containing the same weights of TFC and KBr were prepared.

X-ray measurements were carried out by using Rigaku DMAX 2500 X-ray diffractometer with reflection geometry and C_uK_α radiation (wavelength $\lambda = 1.54$ Å) operated at 40 kV and 100 mA. Data were collected within the range of scattering angles (2θ) of $2 \sim 30°$.

Transmission electron microscopy (TEM) images were obtained using a TEM 2000 EX-II instrument (JEOL, Tokyo, Japan) operated at an accelerating voltage of 100 kV to observe the nanoscale structures of the various composites. All of the ultra-thin sections (less than 100 nm) were microtomed using a Super NOVA 655 001 instrument (Leica, Swiss) with a diamond knife at liquid nitrogen temperature and were then subjected to TEM observation without staining.

Melt rheological measurements were conducted on a rotational rheometer (Physica, MCR 300, Stuttgart, Germany). Dynamic oscillatory shear measurements were performed by applying a time dependent strain of $\gamma(t) = \gamma_0 \sin(\omega t)$ and the resultant shear stress of $\sigma(t) = \gamma_0 \ [G' \sin(\omega t) + G'' \cos(\omega t)]$, where G' and G'' being the storage and loss modulus, respectively. Measurements were conducted by using a set of 25 mm-diameter parallel plates with a sample thickness of 1 mm. The strain amplitude was fixed to

1 % to obtain reasonable signal intensities to avoid the nonlinear response.

RESULTS AND DISCUSSION

Functionalization of the organoclay

GPS and MPS monomers [$RSi(OCH_3)_3$] contain three hydrolyzable alkoxy groups and an organic chain with an epoxy functional group. The silane compounds were initially immiscible with water. However, in the presence of a small amount of acid or base, the three methoxy groups were hydrolyzed to produce [$RSi(OH)_3$] and a single-phase solution resulted. Addition of an alcohol to the solution enhanced the initial miscibility and therefore speeded up the hydrolysis reaction. Hydrolyzed (or partially hydrolyzed) monomers then underwent condensation reactions to form dimers and oligomers.

Pohl and Osterholtz[8] found that the hydrolysis rate was slower at neutral pH than at either acidic or basic conditions. In contrast, the condensation of [$RSi(OH)_3$] to dimer or oligomers proceeded more slowly at pH 4 than at pH 7. Thus, the hydrolyzed monomers and the low-molecular-weight oligomers remained stable in the solution for hours or even days at about pH 4.

When the silane compounds were added to the ethanol/water solution, a condensation reaction as well as the hydrolysis one took place at the same time. The hydrolyzed monomers and oligomers were adsorbed on the surface of C25A and reacted with the silanol groups on the surface of C25A in parallel. The pH and suspension composition should be well controlled to induce reaction of GPS with C25A and to minimize production of the homocondensates.

Figure 2 shows the FTIR spectra of C25A and GPS-modified C25A. C25A was characterized by broad and strong peaks at *ca* 900–1149 cm^{-1}. The peak for Obond;H stretching of Si–OH appeared at 3638 cm^{-1}. The sharp absorbances at 1118 and 1040 cm^{-1} were assigned to Si–O stretching while the peaks at 916 and 881 cm^{-1} were due to Al–O–H stretching.[9] The presence of two bands near 525 and 471 cm^{-1} came from Al(Mg)–O–Si stretching. The strong absorbance at 1087 cm^{-1} originated from $Si–O–CH_3$ stretching vibration.[10] The weak band at 797 cm^{-1} was assigned to Si–O–Si deformation. The peaks for C–H stretch of the aliphatic groups of the O–clay appeared at 2919 and 2850 cm^{-1}.

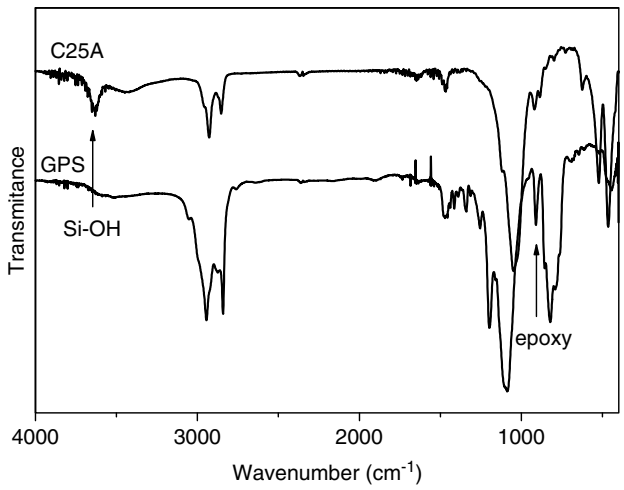

Figure 2. FTIR spectra of C25A and GPS-nodified C25A.

Clay exhibits net negative charge on its lamellar surface, which enables it to adsorb cations, such as Na^+ or Ca^{2+}, and occupies the gallery space between the nano-scaled layers in the naturally occurring mineral.[11] Because the negative charge originates in the silicate layer, the cationic head group of an alkylammonium molecule preferentially resides at the layer surface with the aliphatic tails being removed from the surface. The presence of these aliphatic chains in the galleries alters the original silicate surface from being hydrophilic to organophilic.

However many Si–OH groups still remain on C25A surface even after the organophilic modification. These hydroxyl groups reacted with GPS and MPS to introduce epoxy functional groups and to increase organophilicity, which would increase wetting of the clay layers with the polymer matrix. Physical properties of the polymeric composites with TFC were expected to be better than those with pristine C25A.

The chemical bonding of the silane compounds to C25A can be confirmed through the FTIR observation. Figures 3 and 4 show the change in

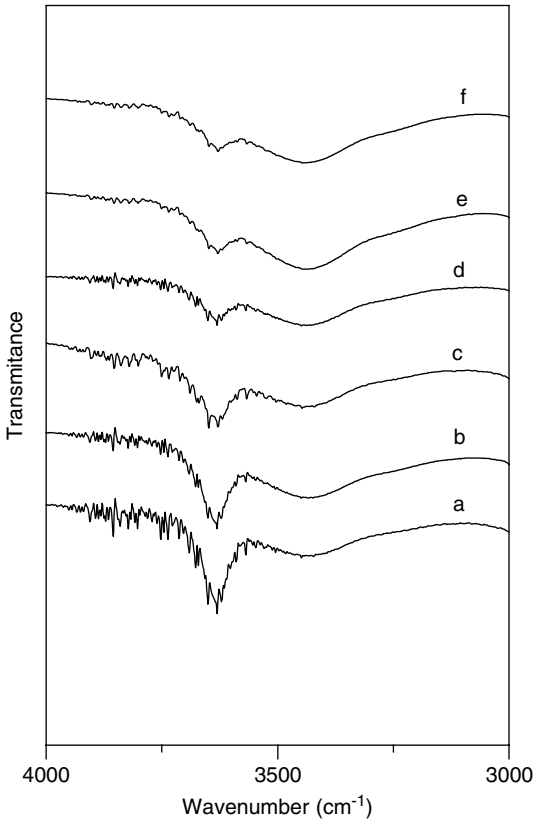

Figure 3. FTIR difference spectra of Cloisite 25A treated with glycidyloxypropyl)trimethoxy silane (GPS) for various periods of time at pH 4 with GPS/C25A = 0.5 wt/wt: (a) Cloisite 25A only, (b) 1 h, (c) 4 h, (d) 8 h, (e) 12 h, (f) 24 h.

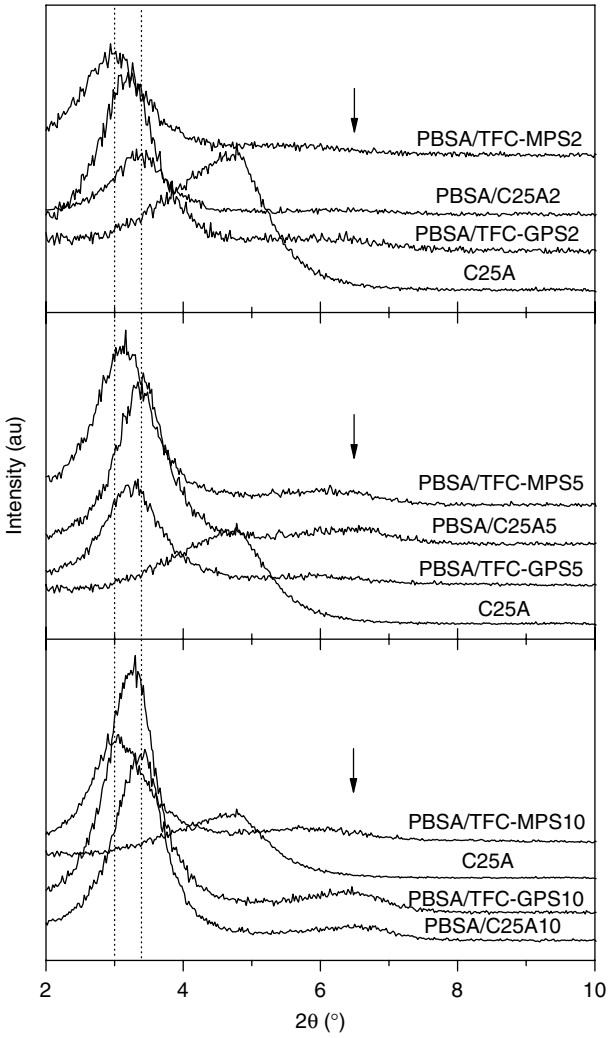

Figure 4. X-ray diffraction patterns of Cloisite 25A®/PBSA composites with the different coupling agents.

the FTIR difference spectra of the clay as a function of time of reaction with GPS at pH 4. IR peaks corresponding to various groups in C25A would remain almost unchanged if the silane molecules were physically adsorbed on the surface of C25A. In contrast, chemical bonding of the silane molecules to C25A would change the IR spectra significantly.[12] Thus, the IR spectra can provide interesting information regarding the chemical bonding between C25A and the silane compound.

It can be seen in Fig 3 that the intensity of the peak at 3638 cm^{-1}, which was assigned to the stretching of terminal Si–OH on the surface of C25A, decreased as the time of reaction of GPS with C25A increased, reaching an asymptotic value of intensity after 12 h of reaction. This confirms the occurrence of the chemical reaction of the hydrolyzed GPS monomers or oligomers with the silanol groups of C25A. According to Xue *et al*,[13] more than 90 % of the epoxy rings would remain intact without ring opening after 24 h of the reaction at similar conditions. The silane compound having methacrylate groups (MPS) was chemically linked onto the surface of the clay through the same mechanism as that for the immobilization of the silane compound having epoxy group (GPS) on the surface of the clay.

Therefore it can be said that twice-functionalized organoclay (TFC) containing functional groups was successfully prepared. The functional group could react with the functional end-groups of polyesters,[14] such as PBSA.

Microstructure and morphology of the composites

The intercalation of polymer chains increased the interlayer spacing relative to that of C25A, shifting the X-ray diffraction peak toward a lower angle corresponding to the layer gallery height of the intercalated composites. The interlayer spacing was calculated from the angular position 2θ of the peak by using the Bragg formula.

In case of the composites containing 2 wt% of clay, the d spacing between the layers expanded from 1.85 nm for C25A to 2.64 nm for PBSA/C25A2, 2.79 nm for PBSA/TFC–GPS2, and 3.01 nm for PBSA/TFC–MPS 2, respectively. The number after the abbreviation of PBSA/C25A, PBSA/TFC-GPS and PBSA/TFC-MPS refers to the weight percentage of the respective clays compounded with PBSA. As the content of the clay increased, the 2θ peak became stronger and gradually shifted toward higher diffraction angle at $2\theta = 3.42°$ (2.58 nm) for PBSA/C25A10, $2\theta = 3.22°$ (2.74 nm) for PBSA/TFC–GPS10, $2\theta = 2.96°$ (2.81 nm) for PBSA/TFC–MPS10, respectively. The small peak at $2\theta = 6.3°$ was due to the (002) plane of the clay. The XRD data are showed in Table 1.

The increase in d spacing compared with that of C25A indicates some of the PBSA molecules were inserted into the interlayer of C25A. The lower 2θ angle for PBSA/TFC–MPS and for PBSA/TFC–GPS than for PBSA/C25A reveals that PBSA molecules intercalated into TFC–GPS and TFC–MPS more easily than into C25A, even though the chain length of MPS and GPS was much shorter than that of the organophilic modifier, $[(CH_3)_2HTN^+ (C_8H_{17})]$ used for preparation of C25A.

Table 1. XRD data of PBSA/clay nanocomposites

	Diffraction angle (2θ) and interlayer (d) spacing for percentage of treated clay/copolymer			
Nanocomposite	100/0	98/2	95/5	90/10
PBSA/C25A				
2θ (°)	4.78	3.34	3.42	3.42
d_{100} (nm)	1.85	2.64	2.58	2.58
PBSA/TFC–GPS				
2θ (°)	4.78	3.16	3.20	3.22
d_{100} (nm)	18.46	2.79	2.76	2.74
PBSA/TFC–MPS				
2θ (°)	4.78	2.94	3.08	2.96
d_{100} (nm)	18.46	3.01	2.86	2.81

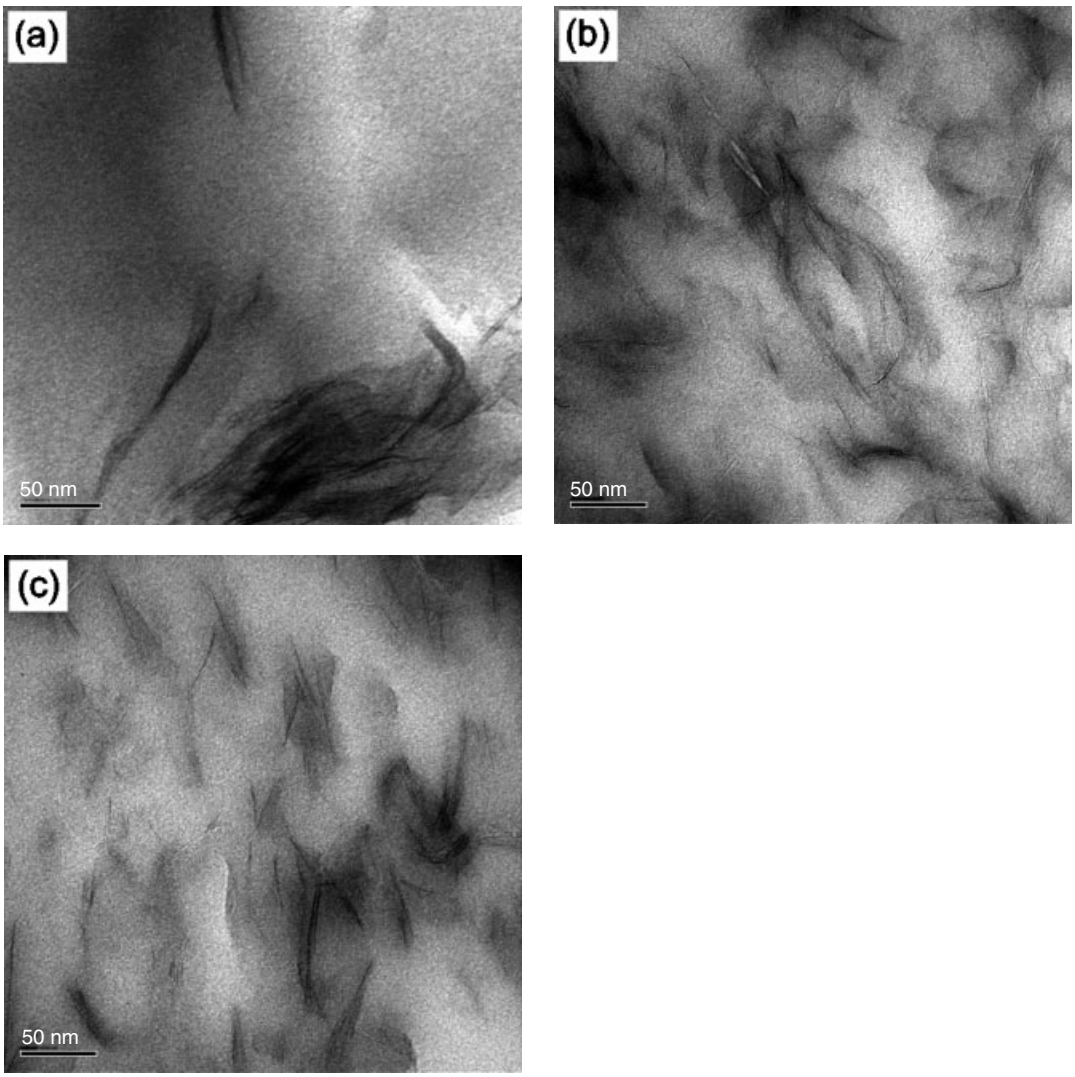

Figure 5. TEM images for PBSA composites: (a) PBSA/C25A5, (b) PBSA/TFC–GPS5, (c) PBSA/TFC–MPS5.

Figure 4 demonstrates that the increase in the *d* spacing of PBSA composite with the MPS-modified C25A is larger than that of PBSA composite containing the GPS-modified C25A. The internal nanometer-scale structure observed by TEM is shown in Fig 5. The dark entities in the TEM images of the composites correspond to the intercalated clay layers. From the TEM results, it can be seen that the stacks of the clay layers forming the clay crystallites were well dispersed in the polymer matrix with multiple ordered platelets,[15] and that the dispersion of the clay layers in PBSA/TFC was better than in PBSA/C25A. These results support the former XRD data. The high degree of exfoliation of the silicate layers and thus high *d* spacing in PBSA/TFC are attributed to the enhanced interaction of TFC with PBSA. Reaction between the end-groups of PBSA and the epoxy groups on TFC–GPS and the polar interaction between the ester groups in TFC–MPS and PBSA should have made a contribution to the enhancement of compatibility.

Rheological behavior of the composites

The linear storage moduli, G', of PBSA, PBSA/C25A, and PBSA/TFC–GPS are shown in Fig 6. The slope of the plot of logarithm of G' as a function of logarithm of angular velocity in the terminal region is listed in Table 2. Owing to the elastomeric nature of PBSA, the slope corresponding to PBSA was 1.31, which was smaller than the slope observed in the homopolymer in general ($G' \propto \omega^2$).[16]

Figure 6 shows that G' of PBSA/TFC–GPS system was much higher than that of PBSA/C25A especially in the low frequency region. G' deviated from that of neat PBSA more significantly at low frequency region as the content of TFC in the composite increased. PBSA/C25A10 and PBSA/TFC–GPS 10 showed non-terminal behavior

Table 2. Slope of G' in the terminal region of PBSA and nanocomposites

Samples	Slope of G'
PBSA	1.31
PBSA/C25A2	1.00
PBSA/TFC–GPS2	0.99
PBSA/C25A10	0.46
PBSA/TFC–GPS10	0.21

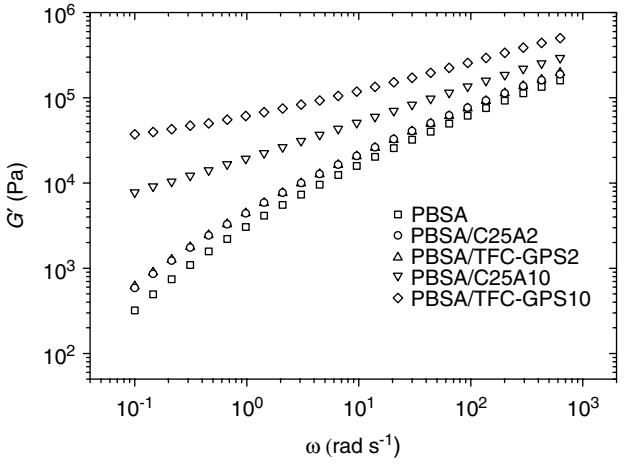

Figure 6. Reduced frequency dependence of the storage modulus, $G'(\omega)$, for PBSA and the composites at $T = 110\,^{\circ}C$.

at the terminal zone. The non-terminal behavior was also observed for other intercalated and exfoliated polymer/clay composites.[17–20] Such behavior was monitored for the composites with solid fillers having a high aspect ratio at high volume fraction, or with solid fillers interacting strongly with the polymer matrix.[21]

According to Table 2, the slope of the plot in Fig 6 decreased with increase in the clay loading and the decrease of the slope was more pronounced for PBSA/TFC–GPS than for PBSA/C25A. Galgali *et al*[22] has attributed the observed behavior of G' to strong solid–solid interactions in the nanocomposites. The aspect ratio of the particles in the nanocomposites reported here was very high and the percolating network was formed at a relatively low volume fraction of the clay. Interaction between the polymer matrix and TFC–GPS was certainly enhanced greatly through the reaction between the epoxy groups of TFC–GPS and the end-groups of PBSA.[14]

Mechanical properties

Table 3 sets out tensile properties of the composites containing different amount of the clays. Tensile strength at break was enhanced as a result of incorporation of the clays and exhibited a maximum value and then decreased as the clay loading increased. The maximum value of the tensile strength at break was 18.7 MPa when the content of C25A was 5 wt%. PBSA/TFC–GPS and PBSA/TFC–MPS composites showed the maximum value of the tensile strength at break of 20.9 MPa when the content of TFC–GPS and that of TFC–MPS were 5 wt% and 2 wt%, respectively. Above the clay loading corresponding to the maximum value, the tensile strength at break of all the composites started to decrease. This is due mainly to the agglomeration of the clay particles,[23] because cracks are usually initiated on and propagated through the agglomerates to provoke failure of the specimens.[24] The higher tensile strength of PBSA/TFC–GPS and PBSA/TFC–MPS systems than that of PBSA/C25A should be attributed to the uniform dispersion of the clay particles.

Table 3. Tensile properties of PBSA, PBSA/C25A, PBSA/TFC–GPS and PBSA/TFC–MPS

Sample	Modulus (MPa)	Strength at break (MPa)	Elongation at break (%)
PBSA	163.5	15.6	408.0
PBSA/C25A2	222.1	18.6	439.5
PBSA/C25A5	251.0	18.7	442.5
PBSA/C25A10	248.7	17.5	428.0
PBSA/C25A15	234.0	17.2	380.5
PBSA/TFC-GPS2	226.2	20.0	430.5
PBSA/TFC-GPS5	249.3	20.9	447.0
PBSA/TFC-GPS10	283.8	20.6	419.0
PBSA/TFC-GPS15	381.8	20.4	361.0
PBSA/TFC-MPS2	244.3	20.9	605.0
PBSA/TFC-MPS5	261.7	18.5	438.0
PBSA/TFC-MPS10	296.2	18.2	417.5
PBSA/TFC-MPS15	342.3	17.3	416.5

The tensile modulus of PBSA/C25A composite increased from 163.5 MPa to 251.0 MPa as the content of C25A increased to 5 wt%. Further increase in the C25A loading to 15 wt% reduced the modulus down to 234.0 MPa. In contrast, the modulus of the composites with TFC–GPS and TFC–MPS rose monotonically to 381.8 and 342.3 MPa, respectively, as the clay loading increased to 15 wt%. The significant enhancement of the modulus of the composites with TFC–GPS and TFC–MPS was ascribed to the resistance exerted by the clay itself as well as to the orientation and the higher aspect ratio of the layers[25] owing to the fine dispersion and strong interaction between TFC and PBSA.

Elongation at break of PBSA with either C25A, TFC–GPS or TFC–MPS increased at a low loading of the clay and then decreased with further increase in the clay content. It is curious to observe that elongation at break of PBSA/C25A was not far inferior to that of PBSA/TFC–GPS or to that of PBSA/TFC–MPS in spite of the difference in the degree of dispersion of the clay layers and of the difference in the interaction between the clay layers and PBSA. Further research is needed to elucidate the origin of this peculiar behavior of elongation at break.

Reaction between the end groups of PBSA and the epoxy groups on TFC-GPS is outlined in Scheme 1 and this type of chemical reaction was confirmed by observing the FTIR spectrum of the composite after extraction with boiling chloroform.[26,27]

As cited above, the mechanical properties of PBSA/MPS-modified clay were better than those of PBSA/GPS-modified clay composites in spite of the fact that the MPS-modified clay did not have any functional groups to react with PBSA. The polar interaction between the ester groups should be responsible in part for the better mechanical properties. A further research is under way to further clarify the origin of the improved mechanical properties of the PBSA/MPS-modified clay composites.

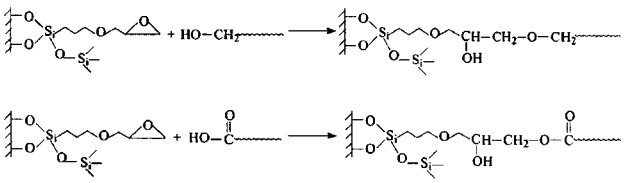

Scheme 1. Reactions between the end-groups of PBSA and the epoxy groups on TFC–GPS.

CONCLUSIONS

A new and convenient method was devised to prepare twice-functionalized organoclay (TFC) by reacting GPS and MPS with the silanol groups of C25A. TFC as well as C25A was melt compounded with PBSA to prepare PBSA/C25A, PBSA/TFC–GPS and PBSA/TFC–MPS composites. The additional functionalization of C25A affected significantly the structure of the composites and the material properties. The linear storage modulus of PBSA/TFC was much higher than that of PBSA/C25A, especially in the low-frequency region, and non-terminal behavior was observed at the terminal zone as a result of the enhanced interaction between PBSA and TFC. Tensile modulus and strength at break of PBSA were greatly improved by compounding with TFC–GPS and TFC–MPS due to the increased interfacial interaction.

ACKNOWLEDGEMENTS

This work was supported by grant No R01-2002-000-00146-0 from the Interdisciplinary Research Program of the KOSEF. The support of post-doctorate fellowship for GXC from the Brain Korea 21 Project in 2003 is gratefully acknowledged.

REFERENCES

1 Ray SS, Yamada K, Okamoto M, Ogami A and Ueda K, *Chem Mater* **15**:1456 (2003).
2 Krishnamoorti R, Vaia RA and Giannelis EP, *Chem Mater* **8**:1728 (1996).
3 Ray SS, Maiti P, Okamoto M, Yamada K and Ueda K, *Macromolecules* **35**:3104 (2002).
4 Gonsalves K and Chen X, in *Materials Research Society Symposium Proceedings*, Vol 435, Materials Research Society, Warrendale, PA, p 55 (1996).
5 Giannelis EP, *Adv Mater* **8**:29 (1996).
6 Chen GX, Choi JB and Yoon JS, *Macromol Rapid Commun* **26**:183 (2005).
7 Freeman SK, *Applications of Laser Raman Spectroscopy*, J Wiley & Sons, New York (1974).
8 Pohl ER and Osterholtz FD, in *Molecular Characterization of Composite Interfaces*, ed by Ishida H and Kumar G, Plenum Press, New York, p 157 (1985).
9 Shen Z, Simon GP and Cheng YB, *Polymer* **43**:4251 (2002).
10 Tesoro G and Wu Y, in *Silanes and Other Coupling Agents*, ed by Mittal KL, VSP Publishers, Utretcht (1992).
11 Alexandre M and Dubois P, *Mater Sci Eng* **R28**:1–63 (2000).
12 Dai JC and Huang JT, *Appl Clay Sci* **15**:51 (1999).
13 Xue G, Koenig JL and Ishida H, *Rubber Chem Technol* **64**:162 (1991).
14 Kim HY, Jeong U and Kim JK, *Macromolecules* **36**:1594 (2003).
15 Vaia RA and Giannelis EP, *Macromolecules* **30**:8000 (1997).
16 Ferry JD, *Viscoelastic Properties of Polymers*, 3rd edn, J Wiley & Sons, New York (1980).
17 Feng W, Kadi A and Riedl B, *Macromol Rapid Commun* **23**:703 (2002).
18 Solomon MJ, Almusallam AS, Seefeldt KF, Somwamgthanaroj A and Varadan P, *Macromolecules* **34**:1864 (2001).
19 Hyun YH, Lim ST, Choi HJ and Jhon MS, *Macromolecules* **34**:8084 (2001).
20 Krishnamoorti R and Giannelis EP, *Macromolecules* **30**:4097 (1997).
21 Han CD, *Multiphase Flow in Polymer Processing*, Academic Press, New York (1981).
22 Galgali G, Ramesh C and Lele A, *Macromolecules* **34**:852 (2001).
23 Chang JH, An YU, Cho D and Giannelis EP, *Polymer* **44**:3715 (2003).
24 Masenelli-Varlot K, Reynaud E, Vigier G and Varlet J, *J Polym Sci, Polym Phys Ed* **40**:272 (2002).
25 Yano K, Usuki A and Okada A, *J Polym Sci, Polym Chem Ed* **35**:2289 (1997).
26 Ju MJ and Chang FC, *J Appl Polym Sci* **73**:2029 (1999).
27 Ashcroft WR, *Chemistry and Technology of Epoxy Resins*, ed by Ellis B, Blackie Academic & Professional.